MO studies of propylene adsorption on $EtInd_2ZrCH_3^+\|SiO_2^*MAO^-$

María Luján Ferreira [a], P. Belelli [a], A. Juan [b], D.E. Damiani [a,*]

[a] *Complejo CRIBABB, Edificio 2 (PLAPIQUI), Camino Carrindanga km 7, Casilla de Correo 717, (8000) Bahía Blanca, Argentina*
[b] *Departamento de Física, U.N.S., Avda Alem 1253, 8000, Bahía Blanca, Argentina*

Abstract

The system $EtInd_2ZrCH_3^+\|SiO_2^*MAO^-$ was studied theoretically by means of an extended Hückel method (EHMO) for the propylene adsorption. The adsorption of the different forms of olefins was evaluated on the active site formed by metallocene and silica, in presence or not of methylaluminoxane (MAO). In this way, it is possible to appreciate the important function of MAO when the active site is modeled considering all components. According to these results the presence of MAO avoids the adsorption of some forms of propylene. © 1999 Elsevier Science B.V. All rights reserved.

1. Introduction

Since many years, organometallic chemists have been using soluble Ti and Zr complexes as model systems for studying the fundamental reactions in the catalytic polymerization of olefins [1,2]. Among these reactions are the generation of a metal site–carbon bond and the repeated insertion of olefins in this bond. The chain transfer reactions to the monomer or to the Al alkyl as well as the hydride elimination reaction are another set of important reactions studied.

The most studied systems are the bis cyclopentadienyl complexes (Cp_2MCl_2; Cp = Cyclopentadienyl; M = Ti, Zr or Hf) that polymerize ethylene in the presence of Al alkyls [3]. Water was usually considered as a poison for these catalysts. However, in 1973 the increase in activity in these systems following the addition of water [4] was made known. Kaminsky postulated that methylaluminoxane (MAO), an oligomer [5] formed by reaction of $(CH_3)_3Al$ and water, causes the increase of activity.

Since 1980 it is known that titanocenes, zirconocenes and hafnocenes (bis ciclopentadienyl and bis indenyl complexes of these transition metals) form with MAO high activity catalysts. Cp_2ZrCl_2/MAO has a very high activity in ethylene polymerization but it is unable to polymerize prochiral olefins in a stereospecific way [6,7]. The discovery in 1984 of the isospecific polymerization of olefins by metallocenes and MAO originated a growing experimental and

* Corresponding author

theoretical investigation on this topic [8,9]. These catalysts not only polymerize with higher activity and stereoselectivity in homopolymerization but they also permit to widen the range of polyolefins produced [9,10].

From a theoretical point of view, one of the most interesting aspects of these catalysts is that the structure of the precursors can be precisely determined. It is relatively easy to correlate the geometrical and electronic properties of the metal complex to the polymer properties. This correlation revealed a great amount of information regarding the polymerization mechanism and the regioespecificity. Theoretical studies using conformational energy calculations of known structures of chiral metallocenes and/or molecular orbital (MO) methods confirmed that the active site is a quasi cationic d^0 metal [2,11]. This site produces isotactic polypropylene through a mechanism that depends on the electronic distribution in the metal and its chirality. The structure of the ligands attached (MAO, indenyls) to the active site controls the insertion of monomer in the metal–carbon bond. The possible role of α-agostic interactions during an olefin insertion at a $[Cp_2Zr(C_2H_4)CH_3]^+$ catalytic center was studied by Prosenc et al. [12]. In that work, alternative reaction modes for α-olefin insertions in a zirconocene alkyl cation were investigated by the extended Hückel method EHMO. Agostic interaction of the Zr center with one α-H atom of the migrating alkyl group was found to stabilize the transition state of the preferred reaction mode. Essential contributions to this preference were identified by fragment MO analysis. The increased rigidity conferred on the insertion transition state by the $Zr \leftarrow H–C$ interaction provides a reasonable explanation for the high degrees of stereoselectivity generally associated with these olefin polymerization catalysts.

The olefin polymerization reaction by silylene-bridged zirconocene catalysts was also theoretically investigated. Using ab initio MO calculations, the structure and energetic of the reactant, the π-complex, the transition state and the product of ethylene insertion into (SiH_2Cp_2)-$ZrCH_3^+$ have been determined. The regioselectivity in propylene polymerization, that is the preference of the catalyst for primary insertion rather than secondary insertion, is well reproduced by the energy difference at the transition state but not by that of the π-complex. It is important to mention that the model excludes the electronic and steric effect of MAO. Regarding the stereoselectivity in isotactic polymerization of propylene by $SiH_2(CpMe_n)_2Zr R^+$, the substitutes on the Cp rings have been found to determine the conformation of the polymer chain end. The polymer end conformation in turn determines the stereochemistry of olefin insertion at the transition state [13]. The regioselectivity has been found in agreement with steric energy at the transition state. If π-complexes are used for comparison, however, one finds the trend opposite to that at the transition state. In the product of the insertion reaction there is a strong $C\beta–H \rightarrow Zr$ agostic interaction. The authors concluded that adaptation of a realistic transition state model is essential for reliable elucidation of insertion mechanisms [13]. Some efforts of optimizing the transition state in the MO–MM mixed approach have been made [14] but some arbitrariness has been pointed out [15]. The same authors have found some trends in the effect of substituents on errors in insertion of olefins [16].

Corradini et al. studied models for homogeneous isospecific Ziegler Natta catalysis. The model site is basically a stereorigid ethylene bis indenyl chiral complex with two ligands (olefin and growing chain). The chiral environment of the metal atom forces the growing chain to choose one or two chiral possible orientations. This in turn allows the chain to discriminate between re or si monomer insertion reaction. The predicted behavior of the model catalytic site seems to be in agreement with presently available experimental data [17,18]. This group concludes that there is a preferred orientation for olefin coordination. In the case of $R,R,EtInd_2TiCl_2$, it is the re position of the

Table 1
Atomic parameters used for EHMO calculation

Atom	Orbital	Orbital exponents	Ionization potentials (eV)
H	1s	1.000	−13.60
C	2s	1.154	−19.65
	2p	1.451	−11.13
O	2s	2.163	−31.6
	2p	2.750	−16.78
Al	3s	1.670	−12.30
	3p	1.383	−6.50
Si	3s	1.60	−20.44
	3p	1.60	−12.41
Cl	3s	2.356	−26.03
	3p	2.039	−14.20
Zr	5s	1.817	−9.870
	5p	1.776	−6.760
	4d	3.835 (0.6211)[a]	−11.18
		1.505 (0.5796)[a]	−11.18

[a] Coefficients used in the double ξ expansion of the d orbitals.

olefin. They confirm the idea that conformational energy calculation can be used as a predictive tool in the study of catalytic systems in which the stereospecificity is mainly determined by non-bonded interactions. Important drawbacks of their calculations are the absence of MAO in the models and not addressing the α-agostic interactions in the transition state proposals. A modified steric environment, taking account of their prompts, would change their results [19]. For instance, according to their figures, there is no room to accommodate an O from the MAO molecule near the Zr atom.

Computational models for site control of stereoregularity in Ziegler Natta catalysis have been limited to rigid model calculation in which only a limited number of torsional angles are varied. The ab initio calculations of Castonguay and Rappé further support the Cossee mechanism in which the polymer flips from side to side [20]. They reported an ab initio study for a zirconium catalyst model system and a molecular mechanics study of the well-known isotactic catalyst $(S,S')C_2H_4(4,5,6,7$-tetrahydroindenyl$)_2ZrCl_2$, the slower atactic meso catalyst, another known isotactic catalyst (S,S') C_2H_4 bis indenyl $ZrCl_2$ and substituted ones.
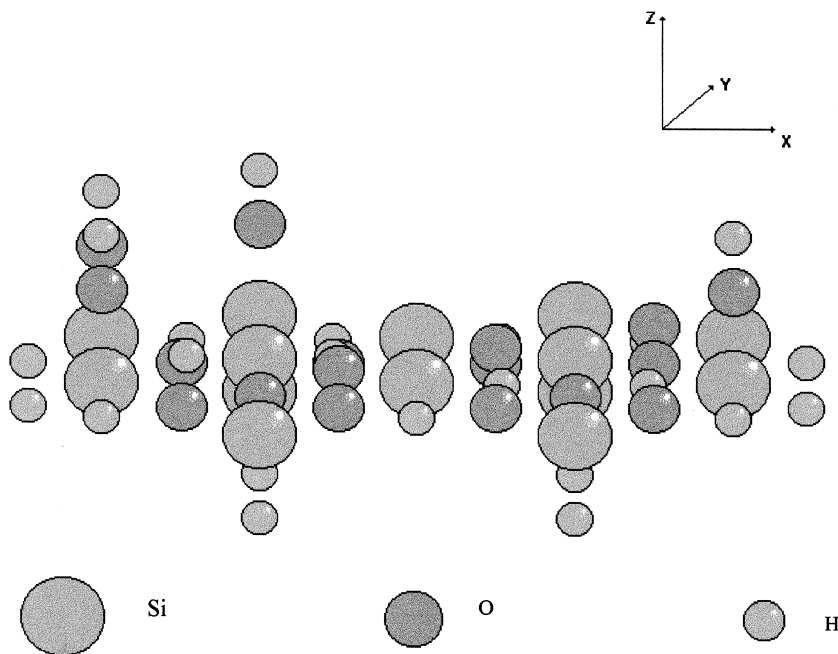

Fig. 1. (111) plane of SiO_2 dehydrated at 600°C.

All these studies have some drawbacks, but one of the most important is that MAO is not considered in the active site structure. So, the steric and geometric effects due to the presence of one (or two) MAO molecule(s) just near the metal center is not considered in the calculations. In this way the results could be different. The need for supporting the metallocenes emerged upon attempting to apply homogeneous systems to full scale polymerization. One of the most interesting supports is SiO_2 that would permit high activity with good control of size and form of the polymer particle. References of theoretical studies of model catalysts including the support and MAO are really scarce.

In the present work the cluster approximation has been used with the extended Hückel method. We study the propylene adsorption on a model of a complete active site (including a local model of MAO) and a support. The support is the (111) plane of SiO_2 as β-cristobalite, modeled after being dehydrated at moderate
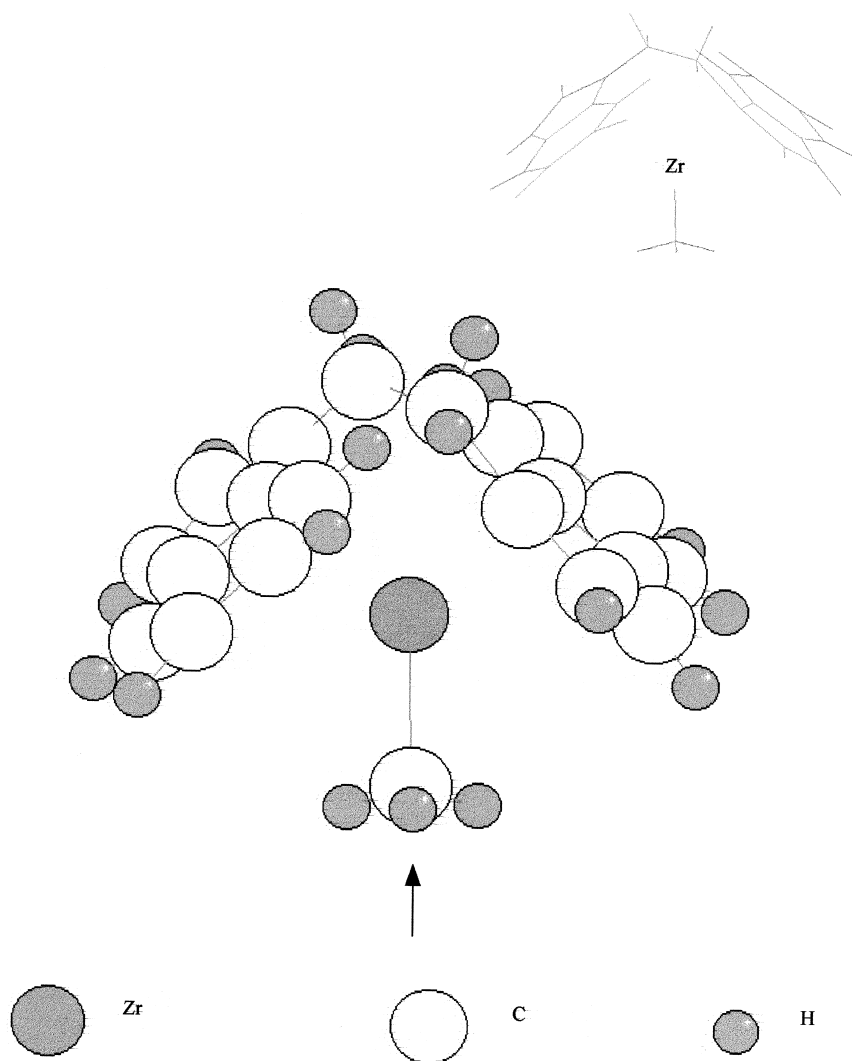

Fig. 2. The cationic alkylated zirconocene.

temperature. We selected a thermally treated plane in order to form siloxane groups on the surface. These would be potential zirconocene adsorption sites.

2. Calculation method

The MO calculations were carried out by means of an extended Hückel modified method (EHMO); a semi-empirical procedure which provides a useful preliminary approach. The EHMO has demonstrated to be a very useful fit approximation to the study of the electronic structure of complex organic and inorganic molecules and has been used for obtaining qual-

itative trends in adsorption processes [21]. In this formalism the non-diagonal elements of one electron extended Hückel Hamiltonian are proportional to the overlap matrix elements. More recently a corrected distance-dependent Wolfsberg–Helmholtz (W–H) formula has been introduced by Calzaferri et al. which solves the problem of the counterintuitive orbital mixing at large bond distances but retains the original idea owing to Anderson and Hoffmann of a distance-dependent W–H constant, in order to improve the calculation of dissociation energies [22,23]. On the other hand, a two body term due to the repulsion between cores has been also added by Anderson to the traditional extended Hückel Hamiltonian [24]. In this approach it has been possible to yield binding energy curves for
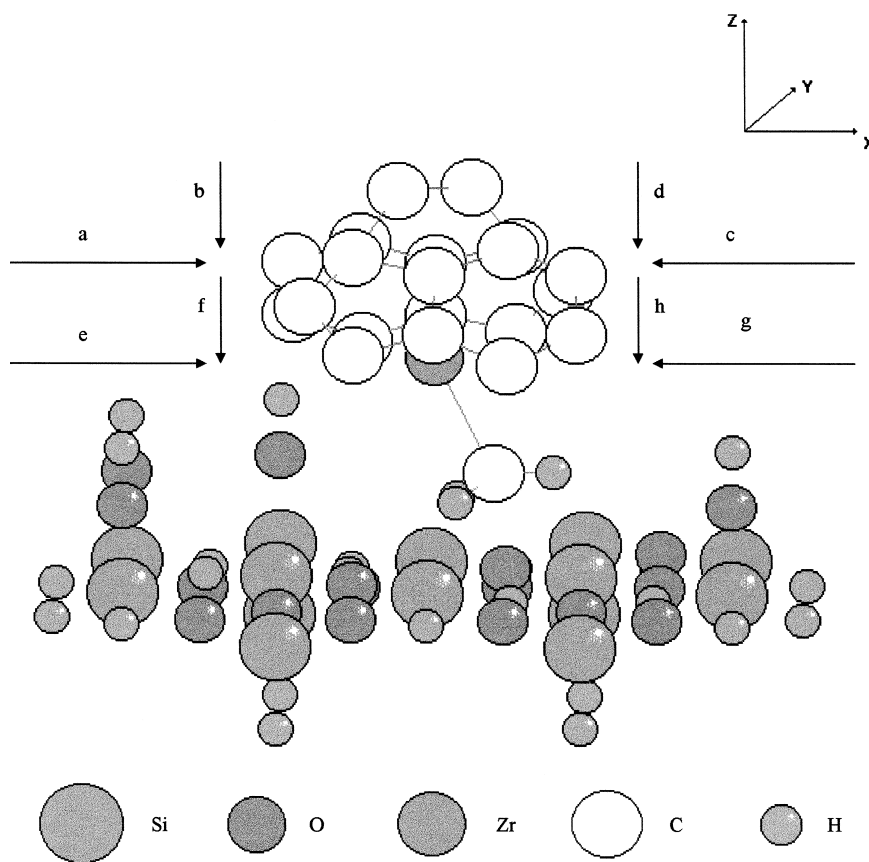

Fig. 3. Model of the active site. Alternative MAO positions considered.

systems of different levels of complexity ranging from bulk metal oxides up to the adsorption of relatively large molecules as benzene on transition metal surfaces [25]. The program used (ICONC) was developed by Kamber et al. [23]. It includes repulsive terms to the total energy which are not explicitly included in the EHMO. In the present work a modified version of the program ICONC developed by Calzaferri et al. has been used. The parameters used have been tested for a series of diatomic molecules and are listed in Table 1. The repulsive coulombic energy is taken into account in a pairwise term.

The total energy (E_t) of our adsorbate/substrate system is expressed as

$$E_t = \Sigma n_i E_i + 1/2 \sum_i \sum_{i \neq j} E_{\text{rep}(i,j)}$$

where the first term corresponds to the attractive valence electrons contribution (n_i) and the second term to the pairwise interatomic repulsions. Each valence level i has an associated energy E_i with occupancy n_i. The repulsion energy of a nucleus i in the presence of a fixed atom j is calculated as an electrostatic term and the summation extended to all possible atom pairs (E_{rep}).
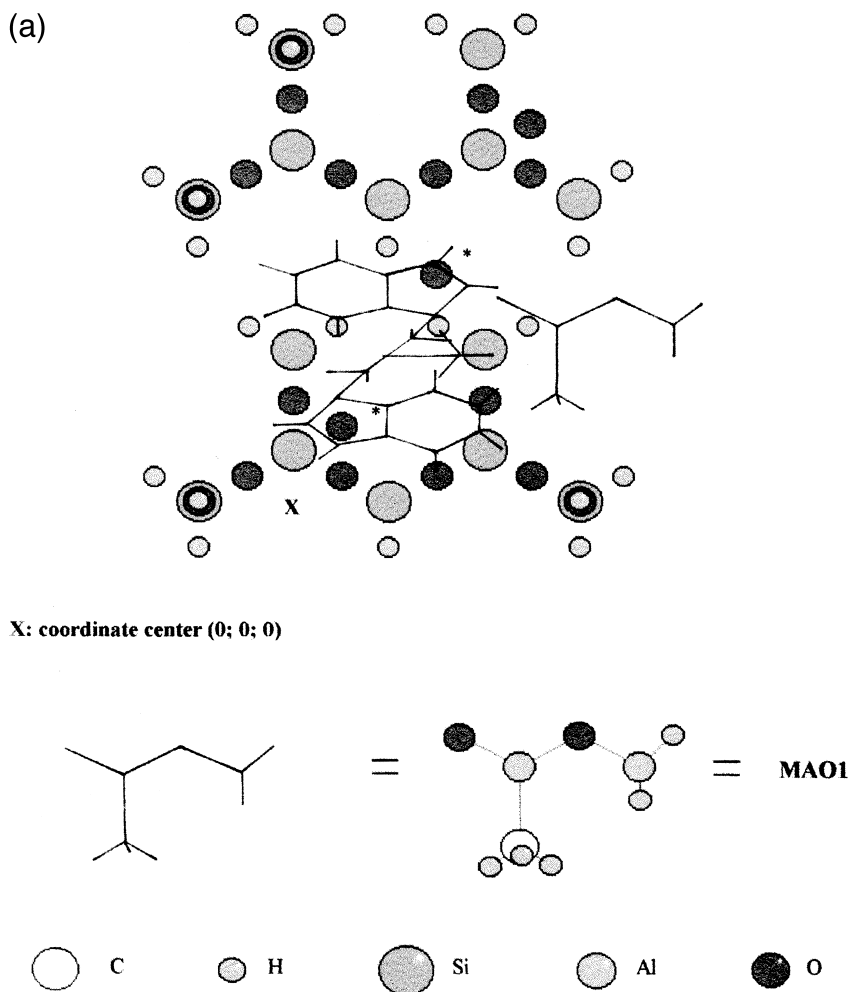
(a)

X: coordinate center (0; 0; 0)

Fig. 4. (a) Top view of the MAO1*S system. (b) Lateral view of the MAO1*S system.
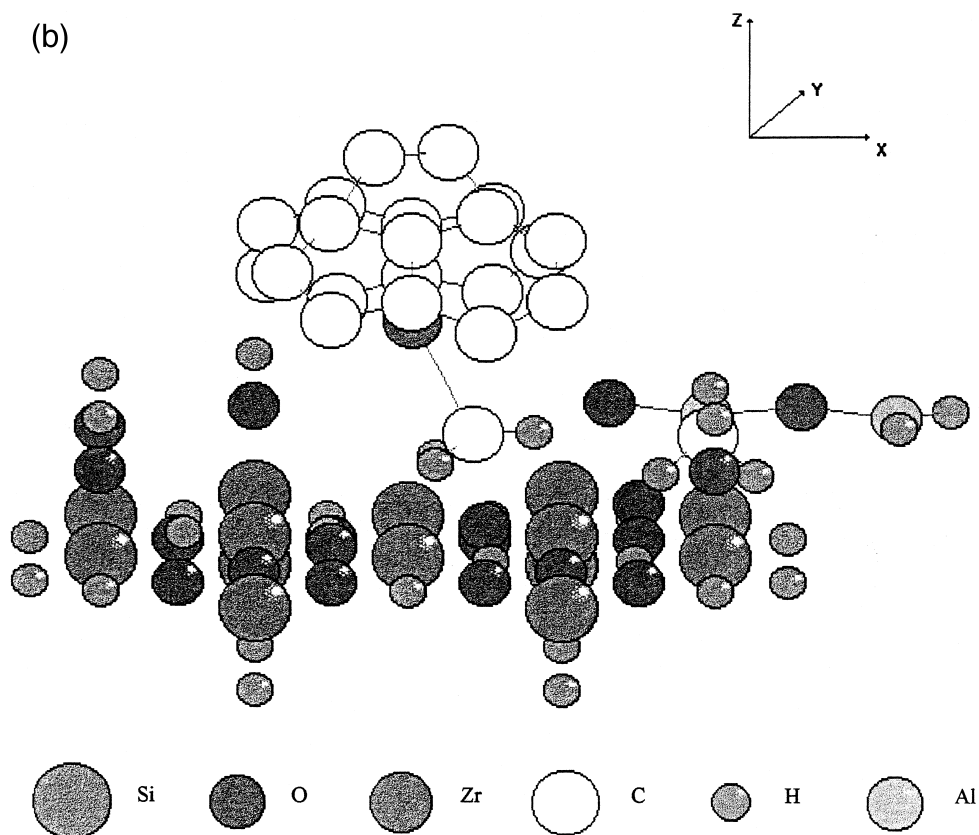
(b)

Fig. 4 (continued).

In our calculation we have used the experimental values for the ionization potentials available from published spectroscopic data [26]. For the level 4p there only exists theoretical data in the literature and therefore we have adopted the data of Hartree–Fock–Slater [27]. With respect to the atomic basic set we have employed a valence set s + p + d of Slater type. The values of the Slater exponents were obtained from the paper of Hoffmann [28].

The total energy of adsorbed species was calculated as the difference between the electronic energy of the system when the adsorbed molecule (propylene) is at a finite distance from the surface and when the molecule is far away from the substrate surface. The geometry optimization was done at 0.1 Å step and due to the approximate nature of extended Hückel like methods the convergence criteria to the energy was set to 0.01 eV.

Our semi-empirical MO calculations have been performed in the framework of the cluster approximation, that is the adsorption site and its neighbourhood was modeled by a portion of the otherwise infinite solid. The section of the cluster and the rest of the lattice result in the appearance of the so-called dangling bonds. It has been observed that while the electron structure converges rather slowly in the bulk limit as the cluster size increases the chemisorption properties are satisfactory predicted [29]. In case of ionic crystals like $MgCl_2$ or SiO_2 there is another source of undesirable effects: the importance of the missing atoms in determining the electric field at the surface. Pisani et al. [30] have performed Hartree–Fock characterization

of the (001) face of α-Al$_2$O$_3$ within the slab approximation. They concluded that a two layer model is nearly adequate for the examination of ionic crystal surfaces. On the other hand, finite size clusters have been used to study adsorption in zeolites [31].

Our research group has performed several calculations on Ziegler Natta systems with the ICONC method with successful prediction of the 2,2,6,6-tetra-methylpiperidine and ethylbenzoate adsorption on MgCl$_2$ and ternary subsequent interactions of these surfaces with TiCl$_4$. We also used this approach with zirconocenes adsorption on MgCl$_2$ and SiO$_2$ as an additional tool to characterize solids that have been previ-

ously experimentally studied by FTIR, XRD, etc. during the different steps of preparation [32–35].

2.1. The surface of SiO$_2$ (111)

Sixty-eight atoms were used to represent the (111) face: 14 Si, 22 O and 32 H (Fig. 1). This plane was chosen because previous work showed that the adsorption of EtInd$_2$ZrCl$_2$ is more stable in this plane than on (100) [32]. Six OHs from silanols groups were condensed, producing three siloxane groups. The surface oxygen atoms obtained after the condensation of the hydroxyl groups were positioned at the same level as Si
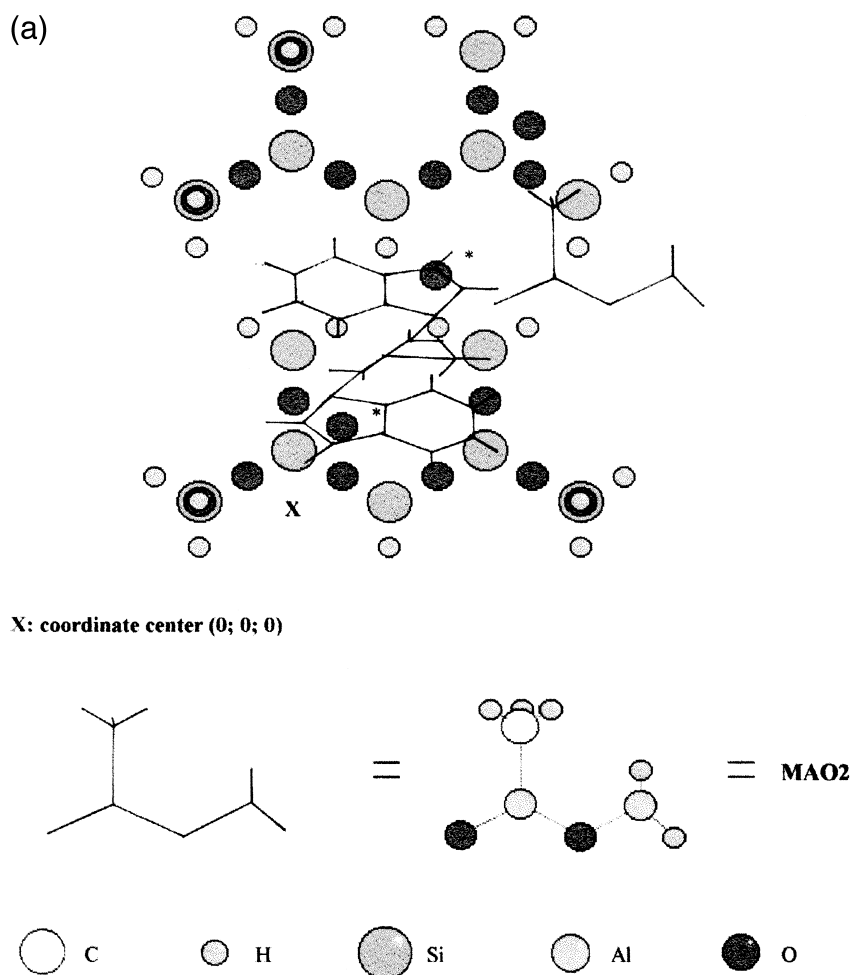

(a)

X: coordinate center (0; 0; 0)

⬡ C　　　◯ H　　　⬤ Si　　　◯ Al　　　● O

Fig. 5. (a) Top view of the MAO2*S system. (b) Lateral view of the MAO2*S system.
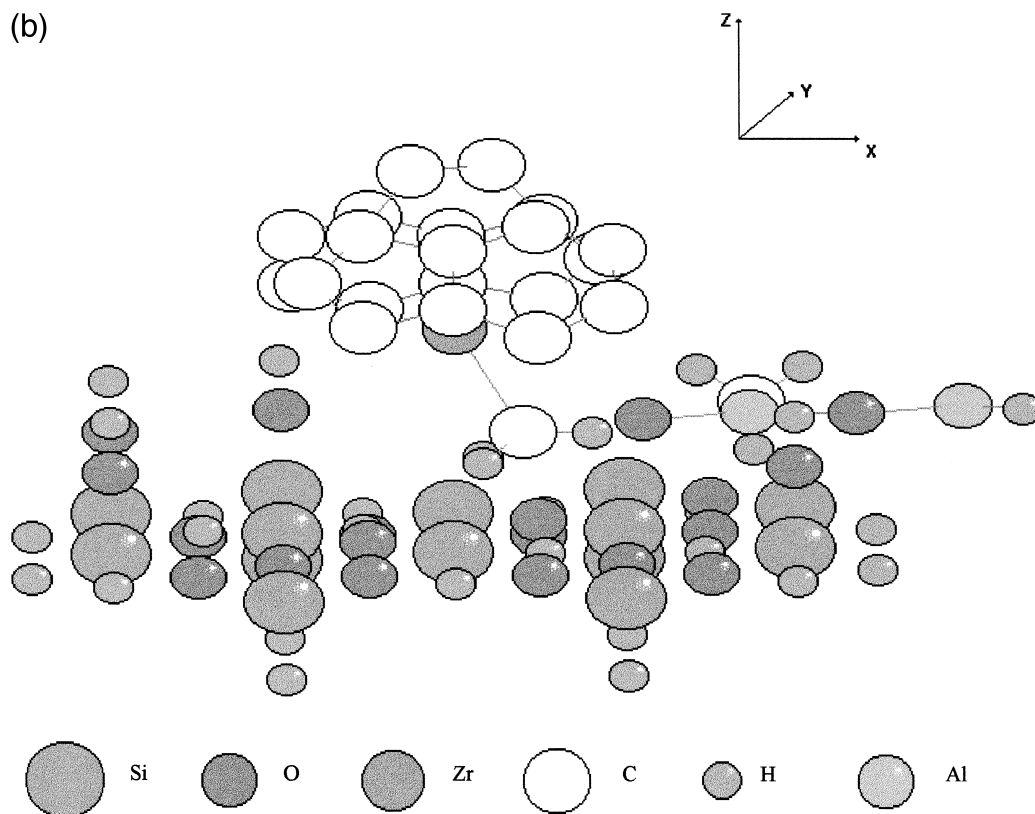
(b)

Fig. 5 (continued).

atoms. This situation was found to minimize the energy. In Fig. 1, the relative size of H, O and Si atoms and their distribution on this plane is shown in a lateral view. In this figure the OH groups are protruding the surface, while siloxanes are in the same plane as that of the Si, leaving room to accommodate the active site.

2.2. The cationic alkylated zirconocene

The selected zirconocene $(EtInd_2ZrCH_3^+)$ was modeled in the (R, R) racemic form (Fig. 2) following literature data [36,37]. It was modified to model the adsorption and activation by MAO. The zirconocene is adsorbed with the indenyls groups away from surface. In this figure the zirconocene is seen from the CH_3 group. The Zr atom is at 3.857 Å from surface plane defined by the Si atoms, between two O atoms of surface, labeled with (*) in Fig. 3. The Zr–CH_3 bond is in the zx plane forming a 63.4° angle with the surface plane. Here and thereafter, the cluster zirconocene-surface is called 'S'. In Fig. 3 the position chosen for the zirconocene on surface is clarified. In this case the zirconocene molecule is rotated 90° around an axis passing through the Zr atom with respect to the view shown in Fig. 2.

2.3. The counterion

The counterion was modeled as O–Al(CH_3)–AlH$_2$. Bond distances were obtained from literature [38] and the O–Al(CH_3)–O angles were set equal to 120°. This is probably the angle in actual real MAO solutions. The distance between Zr and an O atom of the MAO molecule was obtained by calculation and the position of the counterion, varied to a minimum, was achieved.

Different MAO positions were evaluated:

1. parallel to the surface plane, above and to the left of the Zr atom, as represented by the arrow labeled 'a' in Fig. 3;
2. perpendicular to the surface plane, above and to the left of the Zr atom, as represented by the arrow labeled 'b' in Fig. 3;
3. parallel to the surface plane, above and to the right of the Zr atom, as represented by the arrow labeled 'c' in Fig. 3;
4. perpendicular to the surface plane, above and to the right of the Zr atom, as represented by the arrow labeled 'd' in Fig. 3;
5. parallel to the surface plane, between this plane and the Zr atom, to the left of that atom, as represented by the arrow labeled 'e' in Fig. 3;
6. perpendicular to the surface plane, between this plane and the Zr atom, to the left of that atom, as represented by the arrow labeled 'f' in Fig. 3;
7. parallel to the surface plane, between this plane and the Zr atom, to the right of that atom, as represented by the arrow labeled 'g' in Fig. 3;
8. perpendicular to the surface plane, between this plane and the Zr atom, to the right of that atom, as represented by the arrow labeled 'h' in Fig. 3.

Analyzing the different situations we found that the more stable position of MAO is parallel to the surface, placed between the surface and the zirconium atom, to the right of this atom as represented by arrow 'g' Fig. 3. In this way the
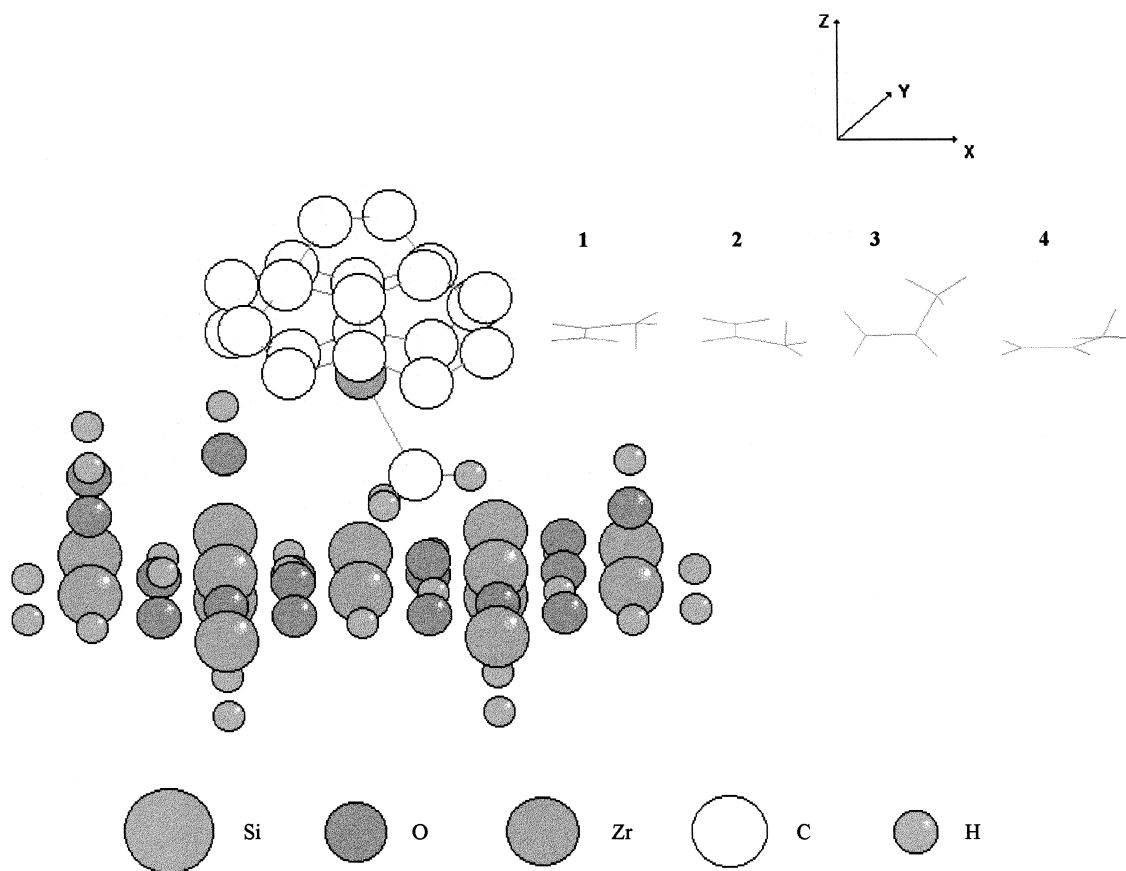

Fig. 6. Propylene adsorption modes on the MAO-modified SiO_2.

Zr atom and the closest O atom belonging to the MAO molecule were 4.12 Å apart. Keeping this distances constant we analyzed two positions.

(1) With the CH_3 group of MAO model oriented towards the same side as the CH_3 group corresponding to the zirconocene molecule. This arrangement is named MAO1. Fig. 4a is a top view of the MAO1*S system were the relative positions of Si, O and H atoms of the dehydrated (111) plane of the surface are clearly shown. The zirconocene molecule, as stated before, is placed between two siloxane groups, marked with an asterisk. Fig. 4b is a lateral view of the same MAO1*S system.

(2) With the CH_3 group of MAO and the CH_3 group of the zirconocene oriented towards opposite sides. This is called MAO2 and its relative position with respect to the metallocene molecule is shown as a top view of the whole system, MAO2*S in Fig. 5a. A lateral view is given in Fig. 5b.

2.4. The propylene

The propylene molecule was modeled with all H atoms included and with the appropriate angles. Four positions of propylene were analyzed with and without counterion following criteria of minimal repulsion. They were identified as PROP1, PROP2, PROP3 and PROP4, respectively, and they are shown in Fig. 6 which also shows the zirconocene-surface cluster S.

2.5. The adsorption of propylene on surface

The adsorption of all forms of propylene was considered not only on the zirconocene-surface cluster S but also on the MAO modified surface MAO*S. The cases analyzed were:
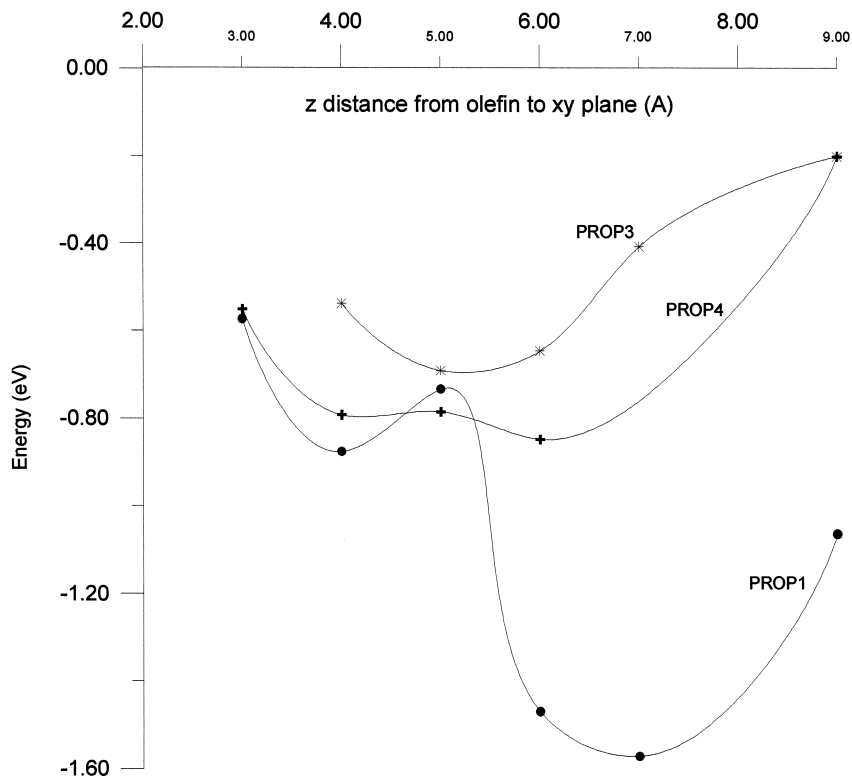1. PROP1*S;
2. PROP2*S;
3. PROP3*S;
4. PROP4*S;

Fig. 7. Results for propylene adsorption on the zirconocene–SiO$_2$ cluster S.

5. PROP1.MAO*S;
6. PROP2.MAO*S;
7. PROP3.MAO*S;
8. PROP4.MAO*S.

The C=C double bond of propylene was fixed at $y = 4.38$ Å (same y coordinate as the zirconocene Zr atom) for PROP1 and PROP2 forms while it was placed at $y = 6.38$ Å for PROP3 and PROP4 in order to facilitate the interaction between the olefin and the zirconocene. Once the y coordinate was fixed for the reasons given above, the olefin position was varied along x and z coordinates. Firstly, the z coordinate was fixed at the same value as the Zr atom z coordinate, then with y and z coordinates fixed the x coordinate was explored until a favorable position was found. Secondly, with the olefin molecule placed at the pair $(x; y)$ where that favorable position was found, the z coordinate was changed until a minimum energy was detected.

When the system PROP.MAO*S was studied, the olefin centroid position was located at the z coordinate where the minimum energy position was observed for the case of the MAO-free surface while simultaneously varying the x and y coordinates. Once the minimum energy position was obtained, the position of the olefin molecule was varied along the z-axis in order to verify the coordinates of the minimum energy position.

In all cases the criteria adopted to choose a new set of coordinates where based on the reasonability of the position in terms of repulsion of the incoming olefin molecule by the zirconocene–MAO-surface system.

3. Results

3.1. Propylene adsorption on the zirconocene-surface cluster S

Results are summarized in Fig. 7 where the energy of the system is plotted against the distance of the centroid of the olefin double bond to the surface plane.

For PROP1*S a shallow minimum is found at $z = 4$ Å $(-0.87$ eV) which can be found after climbing an energy barrier of ~ 20 kcal/mol. The interaction is favorable, even at long distances from the surface.

For PROP2*S (not shown in Fig. 7) the interaction is always repulsive.

In the case of PROP3*S the minimum was found at $z = 5$ Å. The adsorption is stable although the energy involved is lower $(-0.696$ eV) than for PROP1*S.

When the olefin is positioned as in PROP4*S, the minimum is at $z = 6$ Å, where the energy is -0.847 eV.

Table 2
Results for propylene adsorption on MAO*S

Al-olefin distance (Å)	Adsorption energy (eV)	Distance Zr-olefin (Å)
*PROP1.MAO1 * S*		
1.73	6.22	5.24
2.21	−2.14	5.22
2.50	−2.82	
2.64	−2.54	6.13
2.86	−2.10	6.13
3.37	−2.28	6.21
*PROP2.MAO1 * S*		
2.44	2.08	4.13
2.46	−0.30	5.13
2.64	−2.57	6.13
2.86	−2.33	6.13
3.37	−1.91	6.21
*PROP1.MAO2 * S*		
1.73	2.25	5.95
2.21	−2.97	5.94
2.39	−2.84	5.51
2.92	−1.79	5.23
3.26	−1.25	6.21
3.66	−1.65	5.13
4.72	−0.74	6.13
*PROP2.MAO2 * S*		
1.73	5.04	5.95
2.21	−3.65	5.94
2.39	−3.47	5.51
2.92	−2.71	5.23
3.66	−2.65	5.13
4.05	−0.05	4.16
4.48	−2.24	5.13

These results indicate that the most probable form of adsorption of propylene on the zirconocene-surface cluster is PROP1 although PROP3 and PROP4 are also possible. Therefore, it is plausible that propylene approaches as PROP3 or PROP4 and close to the surface changes to PROP1. PROP3 and PROP4 are more stable than PROP1 when they are considered far away from the surface [35].

3.2. The adsorption of propylene on MAO*S

The propylene adsorption was evaluated on the active site that includes the model of MAO (either MAO1 or MAO2). In both cases the distance from the Zr atom to the closest O atom

of the MAO molecule is 4.12 Å. The adsorption of the olefin in its PROP3 and PROP4 forms on the MAO*S system are not allowed due to the high repulsion between propylene and the CH_3 group of MAO. In the case of PROP3 the repulsion of the methyl group of the olefin and the indenyl ligands makes the adsorption unstable in this form. MAO cooperates to avoid a positive interaction. The C=C double bond in PROP4 is not perpendicular to the Zr position and, therefore, the adsorption is unstable [17,39].

The results of EHMO calculations for PROP1.MAO1*S, PROP1.MAO2*S, PROP2.MAO1*S and PROP2.MAO2*S are given in Table 2 where the energy is given as a function of the distance between the olefin and the Al atom bonded to the methyl group in the
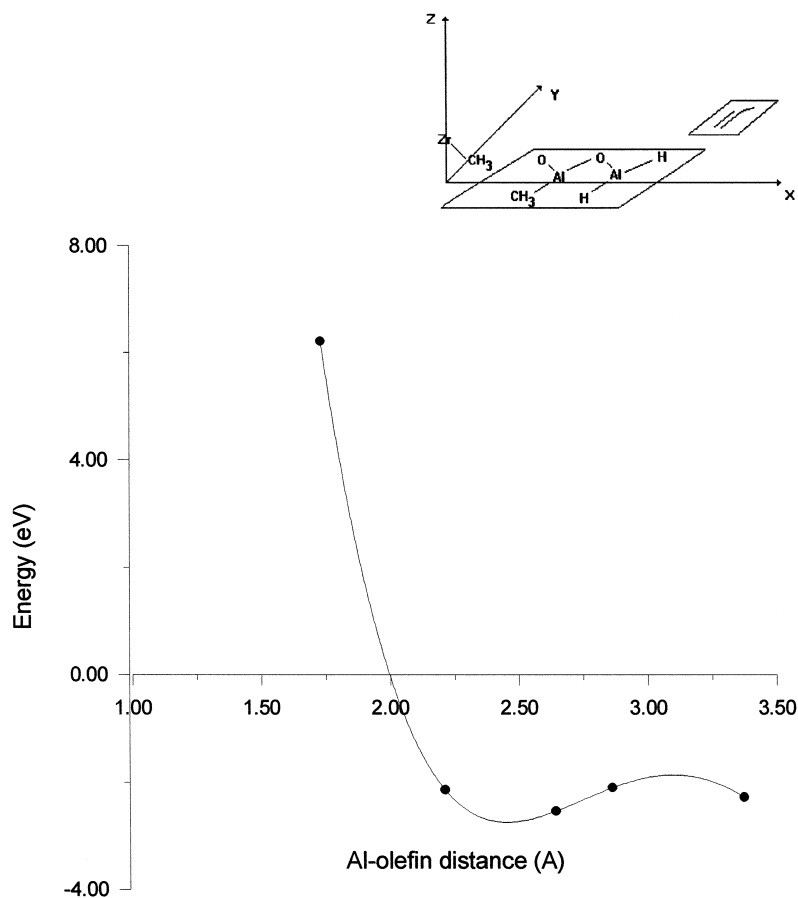

Fig. 8. Propylene adsorption in its PROP1 form on the MAO1*S cluster.

MAO molecule and the distance of the olefin to the Zr atom.

According to these results, which are represented in Figs. 8–11, the adsorption of the olefin onto the MAO1*S cluster is more favorable in the PROP1 form, although it is also possible in the PROP2 way. On the MAO2*S surface, the contrary is true, although in all cases the adsorption is stabilized at less than 3 Å of separation between the olefin and the Al atom bonded to the methyl group in the MAO molecule. However, in order to get closer to the active site on the MAO2*S cluster the olefin molecule has to surpass a relatively important energy barrier. In analyzing these data, it is

necessary to keep in mind the relative positions of the cyclopentadienyl and the indenyl ligands to the Zr atom.

The EHMO analysis of the MAO*S cluster indicate that the more stable form is MAO1*S. Due to repulsive interactions, the adsorption of propylene on MAO1*S is possible; however, strong steric hindrance prevents the olefin insertion to occur. If MAO1 flips to MAO2, by rotating around of the Zr–O bond, the possibility of insertion increases. This flipping must occur before the interaction with propylene.

The complex PROP.MAO*S, more stable, is formed with MAO2 (-3.65 eV or -2.97 eV) whereas with MAO1, the values are higher
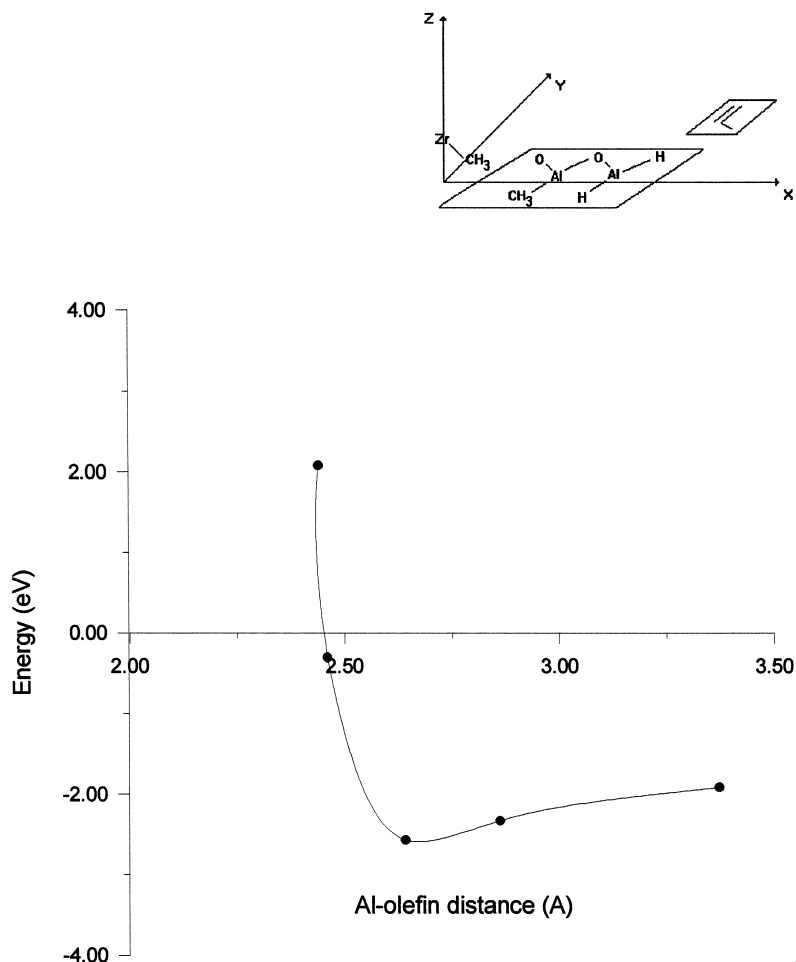

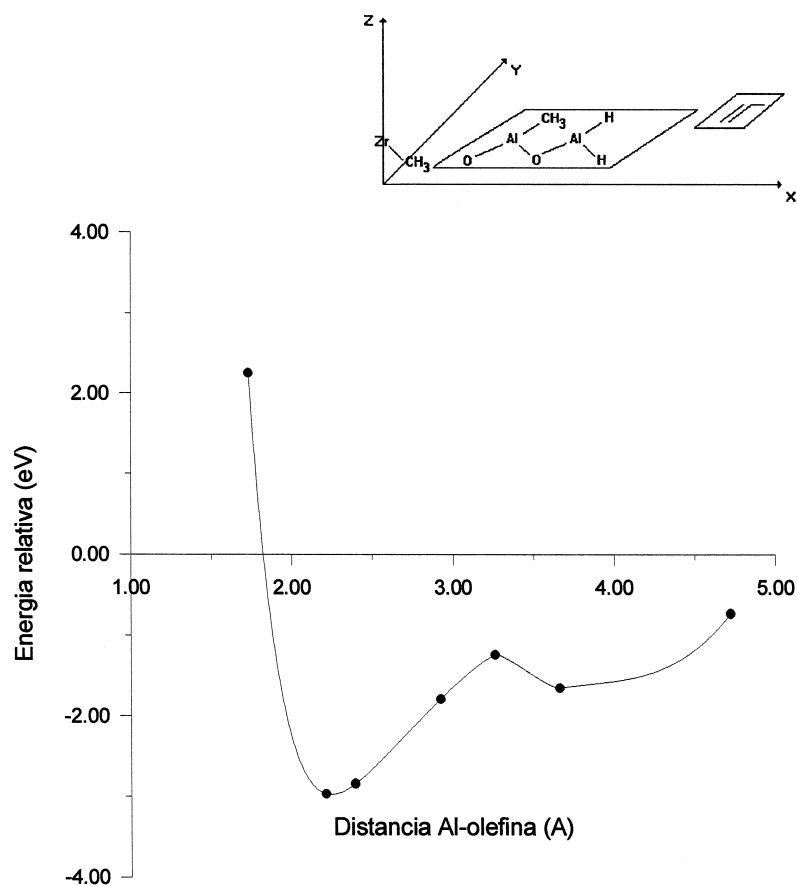Fig. 9. Propylene adsorption in its PROP2 form on the MAO1*S cluster.

Fig. 10. Propylene adsorption in its PROP1 form on the MAO2*S cluster.

(-2.57 eV up to -2.82 eV). As already noted, for PROP1 and PROP2, the energy minima are achieved at approximately the same distance between the olefin and the Al atom bonded to the methyl group in the MAO molecule. On the other hand, almost 6 Å separate the Zr atom from the olefin while the distance between the methyl of the zirconocene and the olefin is close to 5 Å. An important fact is that the bonding energies for PROP1 and PROP2 are greater than the energy of adsorption on surfaces without MAO. A comparison of activation energies and adsorption energies found by calculation is given in Table 3.

PROP1 is the most favorable way for propylene to be adsorbed. In case of MAO1, the insertion will be difficult by steric reasons. In case of MAO2, perhaps the propylene adsorp-

tion on Al is so stable that the insertion will also be difficult.

4. Discussion and conclusions

The first point to consider is the position of the zirconocene on the surface. In the present paper the coordination has been changed from the typical tetrahedral, as it is generally considered (see Refs. [17,18]). In our case the initial coordination number is 5: two indenyls, one CH_3, one O from the SiO_2 surface and the O from MAO (see Figs. 4b and 5b). The coordination of the olefin increases the coordination number up to 6. In this manner the geometrical environment is completely different from the typical MO calculations. The side, that in homo-
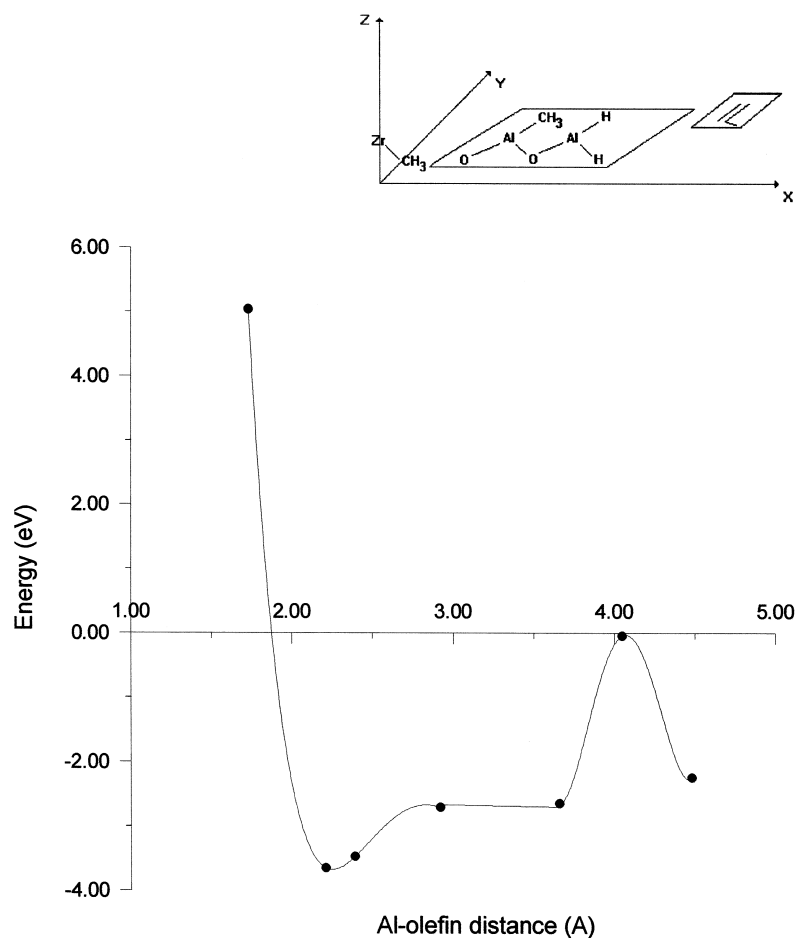
Fig. 11. Propylene adsorption in its PROP2 form on the MAO2*S cluster.

geneous catalysts calculations is used with the alkyl group and the olefin in a supported catalyst model, is occupied by the surface (arrow side of Fig. 2). The orbital description given by Chien et al. [40] justifies the coordination number 5 for Zr: the olefin, both indenyls, the propagating chain and MAO but it does not contain any mention to a support. Whatever the case is, Zr is not tetrahedral. The models used by different groups presented do not take into account the changes produced in orbital description by coordination to MAO and/or the support. Eventually, the coordination number could be increased to 6 if Zr is considered to be bonded to two O atoms of the support.

When the site is modeled without MAO, PROP1 is the more stable form with an adsorption energy of -3.4 kcal/mol. The activation energy in this case is near 17.5 kcal/mol (see Fig. 7). PROP3 and PROP4 are not as stable as PROP1. PROP4 shows no minimum and PROP3 is unstable because it approaches with the methyl group near one of the indenyls (see Fig. 6).

In the models based in homogeneous catalysts, the two chiral coordinations of propylene to $EtInd_2ZrCH_3$ are isoenergetics [18,19]. In our case that is not so. PROP1 is preferred over the rest of the analyzed forms.

In this work we found that the MAO avoids some adsorption ways of propylene when the

Table 3
Activation energy and adsorption energy for propylene adsorption on MAO*S

Activation energy (kcal/mol)	Adsorption energy (kcal/mol)	Figure No.
PROP1.MAO1		
–	−19.6	8
PROP1.MAO2		
14.3	−41.10	10
PROP2.MAO1		
–	−15.6	9
PROP2.MAO2		
52.34	−22.46	11

zirconocene is supported and the active site is modeled complete. When the site is modeled in this way (MAO included) PROP3 and PROP4 are excluded according to our results about adsorption on the bare surface only (see Fig. 7).

When the results on PROP.MAO1*S are analyzed, the minimum distance between the olefin and the Al atom bonded to the methyl group in the MAO molecule is found for both PROP1 and PROP2 to be in the range of 2.5 to 2.64 Å. The adsorption energy for PROP1 is close to −19.6 kcal/mol (see Fig. 8). There is no activation to the adsorption of PROP2 (see Fig. 9) and the adsorption energy is almost −15.8 kcal/mol (see Table 3). PROP1 is preferred over PROP2 when MAO1 is present (see Table 2). When the formation of the site is considered, MAO1*S is more stable than MAO2*S. This could indicate that MAO1*S is formed in higher concentration on this surface.

When the results on PROP.MAO2*S are considered, it can be observed that the adsorption of PROP1 and PROP2 is stronger than on MAO1*S, but it presents an activation energy. The activation energy is larger for PROP2 than for PROP1 (compare Figs. 10 and 11) while the adsorption energy is stronger for PROP1 than for PROP2 (see Figs. 10,11 and Table 3). When the distance Zr-olefin is lowered the repulsion is higher. Steric restrictions support the idea that

MAO1*S easily coordinates the olefin but it does not insert it (see Fig. 4b), because there is no room to accommodate the inserted olefin. In the case of MAO2*S, the adsorption of propylene in the PROP1 form is so stable (see Table 3) that the insertion is difficult too. In case of PROP2 the activation energy is very high (see Fig. 11). In all these cases we are considering the possible adsorption on an Al atom of the MAO group. So the adsorption may be selective on Al (of MAO). The question is that the distance Zr-olefin is very long and the activation energy to get close to bonding distances to Zr is quite high.

These results could explain low productivities (less than 6 kg PP/mol Zrh at 50°C for 1 h at 1 atm) obtained in propylene polymerization using the $EtInd_2ZrCl_2/SiO_2$ MAO system [41]. In this case, the molecular weight of the resulting polymer is approximately 170 000 and the polidispersity is high ($M_w/M_n = 14.8$). There are many sites in these systems. The low yields of polypropylene obtained could be due to the lower reactivity of these species toward propene or to the fact that only part of them is active towards propene [42]. Kaminsky points out that the immobilization of the zirconocene on silica might prevent deactivation by bimolecular process, because the active sites are separated far enough from each other. If even the stereoregularity and specificity are favored by a more stabilized structure (steric interactions) this can explain the product's improved properties (higher molecular weight, isotacticity and melting points of polypropylenes). This author says that an ionic interaction is possible supporting zirconocene on dehydrated SiO_2 like SiO^-Zr^+ where Zr^+ is a cationic species formed from $EtInd_2ZrCl_2$ [43]. Our results confirm these ideas: higher steric hindrance, modified reactivity towards propylene, lower reactivity of these species through a higher activation energy than soluble systems. In soluble systems the activation energy is near 7 kcal/mol. Our calculation predicts at least doubled values for the activation energy (see Table 3).

This work shows that it is very important to consider in the MO calculation the steric and electronic effect of the rest of MAO bonded to the zirconocene cation.

Acknowledgements

References

[1] P. Pino, R. Mülhaupt, Angew. Chem., Int. Ed. Engl. 19 (1980) 857.

[2] R. Jordan, J. Chem. Ed. 65 (1988) 285.

[3] W. Kaminsky, R. Bark, R. Spiehl, N. Moller-Lindenhof, S. Nierdoba, in: W. Kaminsky, H. Sinn (Eds.), Transition Metals and Organometallics as Catalysts for Olefin Polymerization, Springer-Verlag, Berlin, 1988, 291.

[4] K. Reichert, K.R. Meyer, Makromol. Chem. 169 (1973) 163.

[5] J. Herwig, W. Kaminsky, Polym. Bull. 9 (1983) 464.

[6] H. Sinn, W. Kaminsky, H.J. Vollmer, R. Woldt, Angew. Chem., Int. Ed. Engl. 19 (1980) 390.

[7] H. Sinn, W. Kaminsky, Adv. Organomet. Chem. 188 (1980) 99.

[8] J.A. Ewen, J. Am. Chem. Soc. 106 (1984) 6355.

[9] F.R.W.P. Wild, L. Zsolnai, G. Huttner, H.H. Brintzinger, J. Organomet. Chem. 232 (1982) 233.

[10] W. Kamisnky, A. Bark, M. Ardnt, Makromol. Chem. Macromol. Symp. 47 (1991) 83.

[11] P.G. Gassmann, M.R. Callstrom, J. Am. Chem. Soc. 109 (1987) 7875.

[12] M.H. Prosenc, C. Janiak, H.H. Brintzinger, Organometallics 11 (1992) 4036.

[13] H.K. Kuribayashi, N. Koga, K. Morokuma, J. Am. Chem. Soc. 114 (1992) 8687.

[14] A.E. Dorigo, K.N. Houk, J. Org. Chem. 53 (1988) 1650.

[15] M.J. Sherrod, F.M. Merger, J. Am. Chem. Soc. 111 (1989) 2611.

[16] W. Roell, H.H. Brintzinger, B. Rieger, R. Zolk, Angew. Chem., Int. Ed. Engl. 29 (1990) 279.

[17] P. Corradini, G. Guerra, M. Vacatello, V. Villani, Gazzetta Chimica Italiana 118 (1988) 173.

[18] L. Cavallo, G. Guerra, L. Oliva, M. Vacatello, P. Corradini, Polym. Commun. 30 (1989) 16.

[19] L. Cavallo, P. Corradini, G. Guerra, M. Vacatello, Polymer 32 (N7) (1991) 1329.

[20] L.A. Castonguay, A.K. Rappé, J. Am. Chem. Soc. 114 (1992) 5832.

[21] R. Hoffmann, Solids and Surfaces: A Chemist's View of Bonding in Extended Structures, CUCH, New York, 1988, and references therein.

[22] A.B. Anderson, R. Hoffmann, J. Chem. Phys. 60 (1974) 4271.

[23] J. Kamber, L. Forrs, G. Calzaferri, J. Phys. Chem. 93 (1989) 5366.

[24] A.B. Anderson, J. Chem. Phys. 62 (1975) 1187.

[25] A.B. Anderson, J. Mol. Catal. 54 (1989) 281.

[26] W. Lotz, J. Opt. Soc. Am. 60 (1970) 206.

[27] A. Vela, L. Gázquez, J. Phys. Chem. 92 (1985) 5688.

[28] R. Hoffmann, J. Am. Chem. Soc. 107 (1985) 4440.

[29] P.S. Bagus, H.F. Schaefer, C.W. Bauschlinder Jr., J. Chem. Phys. 78 (1983) 1390.

[30] C. Pisani, M. Causa, R. Dovesi, C. Roetti, Prog. Surf. Sci. 25 (1987) 119.

[31] R. Schlieb, D. Heidrich, A. Barth, J. Hoffmann, React. Kinet. Catal. Lett. 10 (1979) 83.

[32] M.L. Ferreira, A. Juan, M.M. Branda, D.E. Damiani, J. Mol. Catal. A: Chem. 122 (1997) 51.

[33] M.L. Ferreira, N.J. Castellani, D.E. Damiani, A. Juan, J. Mol. Catal. A: Chem. 122 (1997) 25.

[34] M.L. Ferreira, D.E. Damiani, A. Juan, Comp. Mater. Sci. 9 (1998) 357.

[35] M.L. Ferreira, A. Juan, D.E. Damiani, React. Kinet. Catal. Lett. 64 (1998) 139.

[36] R.W.P. Wild, G.H. Wasiucionek, H.H. Brintzinger, J. Org. Chem. 288 (1985) 63.

[37] J.L. Atwood, W.E. Hunter, C.H. Duane, E. Samuel, H. Alt, M.D. Rausch, Inorg. Chem. 14 (1975) 1757.

[38] R. Benn, E. Janssen, H. Lehmkuhl, A. Rufinska, K. Angermund, P. Betz, R. Goddard, C. Kruger, J. Org. Chem. 411 (1991) 37.

[39] P. Cossee, J. Catal. 3 (1964) 80.

[40] J.C.W. Chien, B. Rieger, R. Sugimoto, D.T. Mallin, M.D. Rausch, Catalytic Olefin Polymerization, Kodansha, 1989, 565.

[41] M.C. Ferreira, D.E. Damiani, unpublished results.

[42] M.C. Sacchi, D. Zucchi, I. Tritto, P. Locatelli, Macromol. Rapid Commun. 16 (1995) 581.

[43] W. Kaminsky, F. Renner, Makromol. Chem. Rapid Commun. 14 (1993) 239.